

A Quadratic Bending Model for Inextensible Surfaces

Miklós Bergou Max Wardetzky David Harmon Denis Zorin Eitan Grinspun
Columbia University Freie Universität Berlin Columbia University New York University Columbia University

Abstract

Relating the intrinsic Laplacian to the mean curvature normal, we arrive at a model for bending of inextensible surfaces. Due to its constant Hessian, our isometric bending model reduces cloth simulation times up to three-fold.

Categories and Subject Descriptors (according to ACM CCS): I.3.5 [Computer Graphics]: Computational Geometry and Object Modeling

1. Introduction

Computation of curvature-based energies and their derivatives is a costly component of many physical simulation and geometric modeling applications. Typically the energy density is expressed in terms of elementary symmetric functions of the principal curvatures of the mesh [Cia00, YB02, CDD*04, BS05, TW06, GGRZ06]). In general the resulting expressions are nonlinear in the positions of mesh vertices, and the attendant numerics involve costly evaluations of energy gradients and Hessians. Our contribution is to consider the class of isometric surface deformations, arriving at an expression for bending energy which is quadratic in positions. Such quasi-isometric deformations are typical, e.g., for inextensible plates and shells where membrane (stretching) stiffness is greater than bending stiffness by four or more orders of magnitude, hence we focus on cloth simulation as a primary application area.

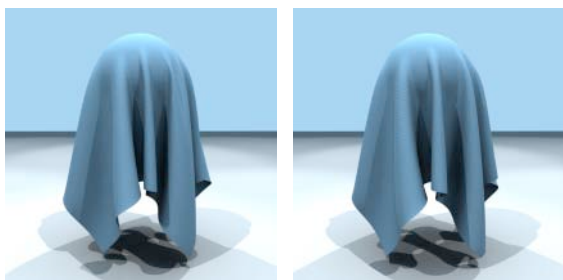


Figure 1: Final rest state of a cloth draped over a sphere, for (left) the proposed isometric bending model and (right) the widely-adopted nonlinear hinge model.

Continuous setting. Consider the bending energy of a deformable surface S :

$$E_b(S) = \frac{1}{2} \int_S H^2 dA, \quad (1)$$

where H is mean curvature and dA is the differential area. $E_b(S)$ is closely related to the Willmore energy of a surface, and the Canham-Helfrich energy of thin bilipid membranes. Note the invariance of $E_b(S)$ under (i) rigid motions and (ii) uniform scaling of the surface: (i) is required for conservation of linear and angular momenta (Nöther’s theorem); (ii) affects the characteristic size of folds and wrinkles.

We may rewrite (1) by the following argument. If $\mathbf{x} : S \rightarrow \mathbb{R}^3$ denotes the embedding of the surface, the mean curvature normal \mathbf{H} of S can be written as the Laplace-Beltrami, Δ , induced by the Riemannian metric of S , applied to the embedding of the surface: $\mathbf{H} = \Delta \mathbf{x}$. Thus we write (1) as

$$E_b(S) = \frac{1}{2} \int_S \langle \Delta \mathbf{x}, \Delta \mathbf{x} \rangle_{\mathbb{R}^3} dA, \quad (2)$$

where $\langle \cdot, \cdot \rangle_{\mathbb{R}^3}$ denotes the standard inner product of \mathbb{R}^3 .

Central observation. The Laplace-Beltrami, Δ , remains unchanged under isometric deformations of the surface—therefore, for inextensible surfaces, $E_b(S)$ is quadratic in positions. Equation (2) together with the assumption of isometric deformation is henceforth called the *isometric bending model* (IBM). Our contribution is to present an analogous *discrete* IBM that is quadratic in positions. Its linear gradient and constant Hessian present an economic model for computing bending forces and their derivatives, enabling fast time-integration of cloth dynamics.

2. Discrete IBM

Our guiding principle for discretization is to maintain the core properties of the smooth isometric bending model. We say that a triangulated surface *deforms isometrically* if its inner metric does not change, *i.e.*, if all edge lengths remain invariant. Denoting the surface’s vertex position vector by $\mathbf{x} = (x_0, x_1, \dots, x_{n-1})^T \in \mathbb{R}^{3n}$, we require our discrete IBM to provide a bending energy $E_b(\mathbf{x})$ which is (i) quadratic in \mathbf{x} under isometric deformations, (ii) invariant under rigid motions of the mesh, and (iii) invariant under uniform scaling. Observing conditions (i) and (ii) we write E_b as

$$E_b(\mathbf{x}) = \frac{1}{2} \mathbf{x}^T \mathbf{Q} \mathbf{x} = \frac{1}{2} \sum_{i,j} Q_{ij} \langle x_i, x_j \rangle_{\mathbb{R}^3},$$

with quadratic form \mathbf{Q} , invariant under isometric deformations, hence depending only on intrinsic mesh properties such as connectivity, edge lengths, inner angles, or area. Since E_b is an energy, \mathbf{Q} must be positive semi-definite. In [BWH*06] we show that condition (ii) is satisfied if and only if $\sum_i Q_{ij} = \sum_j Q_{ij} = 0$. Condition (iii) says that \mathbf{Q} must scale with $1/s^2$ if the whole mesh is scaled by a global factor s . We can then write $\mathbf{Q} = \mathbf{L}^T \mathbf{M}^{-1} \mathbf{L}$, where \mathbf{L} is invariant under scaling and $\sum_j L_{ij} = 0$, whereas \mathbf{M} is symmetric positive definite and scales with s^2 . Like \mathbf{Q} itself, both \mathbf{L} and \mathbf{M} are assumed to only depend on intrinsic mesh properties. A *discrete IBM* is then any energy of the form

$$E_b(\mathbf{x}) = \frac{1}{2} \mathbf{x}^T (\mathbf{L}^T \mathbf{M}^{-1} \mathbf{L}) \mathbf{x} = \frac{1}{2} \mathbf{x}^T \mathbf{Q} \mathbf{x}. \quad (3)$$

The quadratic form $\mathbf{Q} = \mathbf{L}^T \mathbf{M}^{-1} \mathbf{L}$ corresponds to the *constant energy Hessian*.

One way to obtain a suitable \mathbf{M} and \mathbf{L} is to discretize the smooth Laplacian, Δ , using the finite element (FE) method,

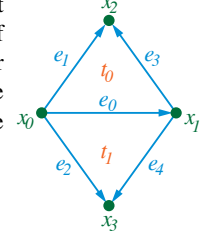
$$L_{ij} = \int_S \langle \nabla \Phi_i, \nabla \Phi_j \rangle dA, \quad M_{ij} = \int_S \Phi_i \cdot \Phi_j dA,$$

where $\{\Phi_i\}$ is some FE basis, the FE stiffness matrix \mathbf{L} is the discrete Laplacian, the FE mass matrix inverse \mathbf{M}^{-1} simplifies to division by area in a lumped mass matrix approximation [ZT00], and $\mathbf{L}\mathbf{x}$ is the discrete analogue of the smooth mean curvature vector, $\Delta \mathbf{x}$.

One possible FE basis is induced by the usual linear Lagrange elements [PP93, CDD*04]. For cloth simulation, where isometric deformations are associated with bending about edges, we prefer non-conforming (edge-based) Crouzeix-Raviart [CR73] elements. As observed by Hildebrandt and Polthier [HP04], in this setting the mean curvature vector, $\mathbf{L}\mathbf{x}$, is associated to edges by construction; in [BWH*06] we show that this version of $\mathbf{L}\mathbf{x}$ corresponds to the *linearization* about the flat (planar) rest state of common mean curvature models used in computer graphics: The models of Bridson *et al.* [BMF03], Cohen-Steiner and Morvan [CSM03], Grinspun *et al.* [GHDS03, GGRZ06], and Bobenko and Schröder [BS05] fall into this category.

Implementation. We present the implementation tools for the Crouzeix-Raviart IBM; for the derivation see [BWH*06]. In a one-time precomputation step, the constant Hessian, \mathbf{Q} , is assembled in the usual manner [ZT00], *i.e.*, by considering contributions from each *local* matrix, $\mathbf{Q}(e_i)$, centered about interior edge e_i with stencil consisting of the triangles, t_0, t_1 , incident to e_i and their vertices, x_0, x_1, x_2, x_3 . With reference to the illustrated labeling convention, we build $\mathbf{Q}(e_0)$ by

$$\mathbf{Q}(e_0) = \frac{3}{2(A_0 + A_1)} \mathbf{K}_0^T \mathbf{K}_0,$$



where A_i is the area of triangles t_i , and \mathbf{K}_0 is the row vector

$$\mathbf{K}_0 = (c_{03} + c_{04}, c_{01} + c_{02}, -c_{01} - c_{03}, -c_{02} - c_{04}),$$

where $c_{jk} = \cot \angle e_j, e_k$. The *local* energy is obtained by $E_b(e_i) = (x_0, x_1, x_2, x_3) \mathbf{Q}(e_i) (x_0, x_1, x_2, x_3)^T$. The *global* (total) energy of the system is obtained by summing over all local contributions corresponding to interior edges.

3. Application to the bending of cloth and plates

We apply the discrete IBM to efficient simulation of clothing and thin plates, which is important for feature film production, fashion design, and manufacturing (see the recent surveys [CK05, MTV05, ZJFP04, NG96]). While resistance to bending is much weaker than to stretching, it is the interplay between the two modes that gives cloth its characteristic folds and wrinkles [TW06, Cia00]. Most models of cloth consider separately the bending and in-plane energies:

$$E(S) = E_b(S) + E_p(S).$$

Since any good model of in-plane response (*e.g.*, [TPBF87, BW98]) satisfies the assumption of small in-plane strains, we view the in-plane model as a mechanism (in the spirit of penalty forces) that enforces isometry. Henceforth, we assume that some in-plane model has been chosen, and we focus on presenting our bending model in the context of a complete cloth solver.

Bending models have been extensively studied in graphics; see Thomaszewski’s recent survey [TW06]. To our knowledge, all popular models are inherently nonlinear in positions, *e.g.*, they may involve expressions in terms of edge lengths or dihedral angles. Some models are linearized every time step, resulting in the lack of Euclidean-motion invariance. The discrete IBM overcomes both of these disadvantages. As a comparison to our IBM, we implemented a “non-linear hinge” model similar to [BW98, BMF03, GHDS03].

Elastic and damping forces. Our elastic and dissipative forces depend on the energy gradient and Hessian, respectively. Elastic behavior is governed by the conservative force

$$\mathbf{f}_e(\mathbf{x}(t)) = -\nabla_{\mathbf{x}} E(S). \quad (4)$$



Figure 2: Snapshots from our simulation of a billowing flag. The accompanying movie demonstrates that despite its economy of cost, the proposed bending model achieves qualitatively the same dynamics as popular nonlinear models.

We model dissipation using the Rayleigh model,

$$\mathbf{f}_d(\mathbf{V}(t)) = -(\alpha_1 M + \alpha_2 \Delta E(S)) \mathbf{V}(t), \quad (5)$$

where $\mathbf{V}(t) = \dot{\mathbf{x}}(t)$ is the velocity, and the damping coefficients α_1 and α_2 govern the decay of low and high frequencies, respectively [ZT00, Hug87]. In implementing IBM, the matrix $-\alpha_2 \nabla^2 E_b(S) = -\alpha_2 Q$ in (5), corresponding to bending, is precomputed once. Similarly, for (4) we compute bending forces via the matrix-vector product $-\nabla_{\mathbf{x}} E_b(S) = -Q\mathbf{x}$. In contrast, the nonlinear hinge requires a relatively expensive computation for both equations.

Dynamics. The time evolution of the cloth is governed by a coupled system of first order initial value problems (IVPs):

$$\underbrace{\begin{pmatrix} \dot{\mathbf{x}}(t) \\ \dot{\mathbf{V}}(t) \end{pmatrix}}_{\dot{\mathbf{q}}(t)} = \underbrace{\begin{pmatrix} Id & 0 \\ 0 & M^{-1} \end{pmatrix}}_A \underbrace{\begin{pmatrix} \mathbf{V}(t) \\ \mathbf{f}_e(\mathbf{x}(t)) + \mathbf{f}_d(\mathbf{V}(t)) \end{pmatrix}}_{\mathbf{b}(\mathbf{q}(t))},$$

given $\mathbf{q}(0)$ and the physical mass matrix M .

Numerical treatment. Time discretization of the above system is a well-studied problem (see [Hau04, BWH*06] and references therein). *Explicit* methods adopt the form $\mathbf{q}_{k+1} = \mathbf{q}_k + h\mathbf{A}\mathbf{b}_k$; here k is discrete time and h is the time step, *i.e.*, $t = hk$, and $\mathbf{b}_k = \mathbf{b}(\mathbf{q}_k)$. *Implicit* methods search for the root of

$$\mathbf{g}(\mathbf{q}_{k+1}) = \mathbf{q}_{k+1} - \mathbf{q}_k - h\mathbf{A}\mathbf{b}(\mathbf{q}_{k+1}) = 0.$$

We solve this nonlinear system in \mathbf{q}_{k+1} with a Newton solver. Letting $\mathbf{q}_{k+1}^{(0)}$ be the initial guess for \mathbf{q}_{k+1} , each Newton iteration improves on the guess,

$$\mathbf{q}_{k+1}^{(i+1)} = \mathbf{q}_{k+1}^{(i)} - (\nabla_{\mathbf{q}} \mathbf{g})^{-1} \mathbf{g}(\mathbf{q}_{k+1}^{(i)}),$$

until convergence. This method requires evaluation of both the energy gradient (to compute \mathbf{g}) and energy Hessian (to compute $\nabla_{\mathbf{q}} \mathbf{g}$), and the IBM provides an efficient way to do so. Finally, it is often desirable to treat some forces explicitly and others implicitly, using IMEX methods [Hau04].

Results. In an evaluation of two solvers, two problem scenarios, two mesh types, and resolutions ranging from 400 to 25600 vertices, we observe a typical two- to three-fold speedup in simulation times compared to the nonlinear hinge. Figures 1-2 and the accompanying movie provide a

visual point of comparison, and Table 1 summarizes our performance measurements. We observe a seven- to eleven-fold speedup in bending force computation. Since IBM's Hessian is precomputed, we can report only the negligible time required to add it to $\nabla_{\mathbf{q}} \mathbf{g}$; in contrast, the repeated computation of the nonlinear hinge Hessian is costly. Overall speedup will depend on the fraction of total computation associated to bending; to estimate this we conducted several experiments:

Experimental setup. We implemented the implicit solver framework of [BW98] as well as the explicit Euler method. The test framework incorporates (i) the constant strain linear finite element for in-plane response [ZT00, Hug87]; (ii) collision detection using k-DOP trees [KHM*98] and response using Bridson's framework [BFA02]; (iii) the PETSc solver library [BGMS96].

Draping cloth. We simulated heavily-damped draping of a square sheet over a sphere (see Figures 1, 3 and the movie). The draped cloths are qualitatively similar in their final configuration and distribution of folds. Only the final draped shape is important, therefore we used large Rayleigh coefficients thus allowing larger time steps [Hug87].

Billowing flag. We simulated the dynamics of a flag under wind (refer to the movie and Figure 2). The billowing motion of the IBM and nonlinear flag are qualitatively similar. We found no need to readjust material parameters when switching from the nonlinear to the IBM model; as discussed in [BWH*06] the carryover of parameters is expected. We modeled wind by a constant homogeneous velocity field, with force proportional to the projection of the wind velocity onto the area-weighted surface normal.

Conclusion. By restricting our attention to isometric deformations—the natural family of deformations for inextensible thin plates—we obtained a bending energy that is quadratic in positions. We demonstrated the consequent performance benefits and the simplicity of implementation in the context of cloth simulation. In [BWH*06] we consider extensions of the theory to anisotropy and curved undeformed configurations (thin shells).

Finally, in [BWH*06] we apply the IBM to fast surface-fairing Willmore flows (see Figure 4). Isometry is a poor assumption in this setting, yet IBM proves effective in the context of inexact-Newton methods.

Draping problem		regular mesh (resolution, in no. vertices)				irregular mesh (resolution, in no. vertices)			
		400	1600	6400	25600	450	2100	6500	22500
Gradient cost (ms)	nonlinear hinge	0.937	3.45	16.4	66.6	1.10	5.43	17.6	67.8
	quadratic IBM	0.081	0.338	2.19	9.15	0.098	0.494	2.32	9.68
Hessian cost (ms)	nonlinear hinge	12.8	54.2	218	890.	15.2	77.2	246	888
	quadratic IBM	0.237	0.963	3.87	15.7	0.266	1.28	3.99	13.6
Explicit step cost (ms)	nonlinear hinge	3.81	6.64	27.5	112.	2.16	9.53	31.4	140.
	quadratic IBM	2.63	2.90	11.9	48.8	0.964	4.35	15.2	76.5
Implicit step cost (ms)	nonlinear hinge	28.6	138	470.	1730	33.9	219	557	1880
	quadratic IBM	11.0	62.7	168	505	13.6	103	219	612

Flag problem		regular mesh (resolution, in no. vertices)				irregular mesh (resolution, in no. vertices)			
		400	1600	6400	25600	450	2100	6500	22500
Gradient cost (ms)	nonlinear hinge	0.975	3.99	16.0	64.0	1.10	5.43	17.8	68.7
	quadratic IBM	0.085	0.341	2.14	8.75	0.099	0.490	2.31	9.28
Hessian cost (ms)	nonlinear hinge	13.4	54.8	212	849	15.2	77.4	247	887
	quadratic IBM	0.251	0.974	3.79	14.99	0.267	1.30	3.96	13.7
Explicit step cost (ms)	nonlinear hinge	1.73	7.05	27.7	112.	1.97	9.80	32.7	134
	quadratic IBM	0.780	3.26	13.3	53.4	0.900	4.54	16.1	70.0
Implicit step cost (ms)	nonlinear hinge	27.6	106	420.	1680	33.5	155	513	1880
	quadratic IBM	9.53	32.9	127	490	12.5	50.4	166	608

Table 1: Computational cost per time step for two solvers, regular- and irregular-meshes, and multiple resolutions, comparing IBM to the nonlinear hinge, as measured on a Pentium D 3.4GHz, 2GB RAM. Time step cost includes collision handling.

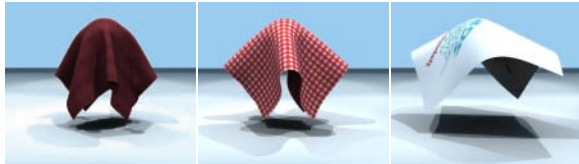


Figure 3: The quadratic bending model is valid over the full range of bending to in-plane stiffness ratios, e.g., (left to right) $10^{-5} : 1$, $10^{-3} : 1$, and $10^{-2} : 1$.

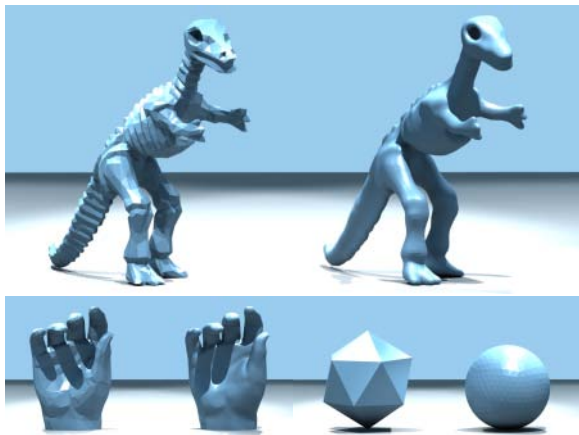


Figure 4: Willmore flow smoothes a dino, a hand and an icosahedron (44928, 24192, and 5120 triangles, respectively). Smoothing requires 7.47s, 4.42s and 120ms, after one-time Hessian factorization costing 8.77s, 5.31s and 200ms, respectively. Flat shaded.

Acknowledgements. This work was supported in part by the DFG Research Center Matheon “Mathematics for key technologies” in Berlin, the NSF (MSPA-MCS 0528402), Elsevier, and nVidia. Special thanks to Konrad Polthier for facilitating the meeting leading to this work, and to Charles Han for his tireless production assistance including lighting and rendering.

References

- [BFA02] BRIDSON R., FEDKIW R., ANDERSON J.: Robust treatment of collisions, contact and friction for cloth animation. *ACM TOG 21*, 3 (2002), 594–603.
- [BGMS96] BALAY S., GROPP W. D., MCINNES L. C., SMITH B. F.: *PETSc 2.0 users manual*. Tech. rep., Argonne National Laboratory, 1996.
- [BMF03] BRIDSON R., MARINO S., FEDKIW R.: Simulation of clothing with folds and wrinkles. *SCA '03* (2003), 28–36.
- [BS05] BOBENKO A. I., SCHRÖDER P.: Discrete Willmore flow. *SGP* (2005), 101–110.
- [BW98] BARAFF D., WITKIN A.: Large steps in cloth simulation. In *Proceedings of SIGGRAPH* (1998), pp. 43–54.
- [BWH*06] BERGOU M., WARDETZKY M., HARMON D., ZORIN D., GRINSPUN E.: Discrete quadratic curvature energies. TR, Columbia University, 2006.
- [CDD*04] CLARENZ U., DIEWALD U., DZIUK G., RUMPF M., RUSU R.: A finite element method for surface restoration with smooth boundary conditions. *CAGD* (2004), 427–445.
- [Cia00] CIARLET P.: *Mathematical Elasticity, Vol III*. North-Holland, 2000.
- [CK05] CHOI K.-J., KO H.-S.: Research problems in clothing simulation. *CAD 37*, 6 (2005), 585–592.
- [CR73] CROUZEIX M., RAVIART P. A.: Conforming and non-conforming finite elements for solving stationary Stokes equations. *RAIRO Anal. Numer.* 7 (1973), 33–76.
- [CSM03] COHEN-STEINER D., MORVAN J.-M.: Restricted Delaunay triangulations and normal cycle. *SoCG 2003* (2003), 312–321.
- [GGRZ06] GRINSPUN E., GINGOLD Y., REISMAN J., ZORIN D.: Computing discrete shape operators on general meshes. *CGF 25*, 3 (2006).
- [GHDS03] GRINSPUN E., HIRANI A. N., DESBRUN M., SCHRÖDER P.: Discrete shells. *SCA '03* (2003), 62–67.
- [Hau04] HAUTH M.: *Visual Simulation of Deformable Models*. PhD thesis, University of Tübingen, 2004.
- [HP04] HILDEBRANDT K., POLTHIER K.: Anisotropic filtering of non-linear surface features. *CGF 23*, 3 (2004), 391–400.
- [Hug87] HUGHES T. J. R.: *Finite Element Method - Linear Static and Dynamic Finite Element Analysis*. Prentice-Hall, Englewood Cliffs, 1987.
- [KHM*98] KLOSOWSKI J. T., HELD M., MITCHELL J. S. B., SOWIZRAL H., ZIKAN K.: Efficient collision detection using bounding volume hierarchies of k-dops. *IEEE TVCG 4*, 1 (January-March 1998), 21–36.
- [MTV05] MAGNENAT-THALMANN N., VOLINO P.: From early draping to haute couture models: 20 years of research. *The Visual Computer 21*, 8–10 (2005), 506–519.
- [NG96] NG H. N., GRIMSDALE R. L.: Computer graphics techniques for modeling cloth. *IEEE CG&A 16*, 5 (Sept. 1996), 28–41.
- [PP93] PINKALL U., POLTHIER K.: Computing discrete minimal surfaces and their conjugates. *Experim. Math.* 2 (1993), 15–36.
- [TPBF87] TERZOPOULOS D., PLATT J., BARR A., FLEISCHER K.: Elastically deformable models. In *Proceedings of SIGGRAPH* (1987), pp. 205–214.
- [TW06] THOMASZEWSKI B., WACKER M.: Bending Models for Thin Flexible Objects. In *WSCG Short Communication proceedings* (2006).
- [YB02] YOSHIZAWA S., BELYAEV A.: Fair triangle mesh generation via discrete elasticity. In *GMP2002* (July 2002), IEEE, pp. 119–123.
- [ZJFP04] ZHU H., JIN X., FENG J., PENG Q.: Survey on cloth animation. *Journal of Computer Aided Design & Computer Graphics 16*, 5 (2004), 613–618.
- [ZT00] ZIENKIEWICZ O. C., TAYLOR R. L.: *The finite element method: The basis*, 5th ed., vol. 1. Butterworth and Heinemann, 2000.